Fundamental Studies on the Microwave Circuits and Electronics

Part. I. The Some Theoretical Studies of Microwave Circuits

By

Nobuyoshi KATO and Toyosaku ISOBE

Department of Electronic Engineering

(Received October 15, 1957)

Abstract

In this paper, the boundary value problems of the microwave circuits such that the junction of the circular wave guides with different radii and the insertion of cylindrical obstacles, i.e, circular hollow dielectric cylinder, metallic post, in a rectangular wave guide etc, are treated and the equivalent circuit representation of each case is introduced.

Introduction and Synopsis

In this paper, some methods of theoretical studies on the boundary value problems of the discontinuity of wave guide as a microwave transmission circuit are treated.

In this first chapter*, the convenient approximate calculations of the boundary value problems at point where the two circular wave guides whose radii are different each other are connected, and the equivalent circuits of this case are introduced.

These results are useful to discussion of the characteristics of a discseal tube cavity, the structure of one of the elements of periodically loaded wave guide of traveling wave tube and discontinuity of the wave guide that transmits the H_{01} mode in the millimeter wave range.

In the second chapter**, how the electromagnetic fields in a rectangular wave guide is disturbed by rather fat cylindrical obstacles inserted into the wave guide, is discussed and its equivalent circuit is introduced. The calculations are performed in the following three cases.

a) The case of a circular hollow dielectric post inserted parallel to the electric field into the wave guide.

---

* This part was published on the Electrical Review of Japan Vol. 38 No. 8 (Oct. 1950).

** This part was published on the Journal of the Institute of Electrical Communication Engineers of Japan, Vol. 38 p. 167 (March 1955).

b) The case in which a metallic post coaxially surrounded by the dielectric cylinder is inserted into the wave guide.

c) The case of a metallic post inserted at variable height into the wave guide.

These results give the theoretical back-ground of a measurement of gap admittance of the tube with a very narrow electrode spacing by wave guide method, in addition to clarify the characteristics of an adjusting screw.

Chapter 1. An Approximate Calculation at the Point of Junction of Circular Wave-guides.

1.1 Introduction

The analyses of the characters of junction of the two wave guides of different radii as shown in Fig. 1.1 in which E_{01} mode or H_{01} mode is propagated are treated and each equivalent circuit is reduced.

1.2 The case in which E_{01} mode is propagated.

An assumption is made that the dimensions of the radii of the both wave guides are so designed that the only lowest modes can be possibly propagated.

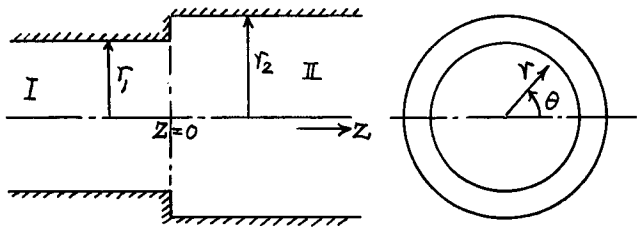

Fig. 1.1. The junction of circular wave guides.

Then the transverse field components of both sides of the junction part the lowest mode is propagated from either one of the two waveguides are expressed in the following equations when time factor $e^{j\omega t}$ is omitted and their formulae are normalized for the convenience of theoretical expansion.

$$\left.\begin{aligned} E_r^{\mathrm{I}} &= a_1^i \frac{J_1\left(\lambda_1 \frac{r}{r_1}\right)}{\sqrt{\gamma_1}} e^{-jh_1 z} + \sum_{l=1}^{\infty} a_l \frac{J_1\left(\lambda_l \frac{r}{r_1}\right)}{\sqrt{\gamma_1}} e^{jh_l Z} \\ E_r^{\mathrm{II}} &= b_1^i \frac{J_1\left(\lambda_1 \frac{r}{r_2}\right)}{\sqrt{\gamma_1}} e^{jh_1 Z} + \sum_{l=1}^{\infty} b_l \frac{J_1\left(\lambda_l \frac{r}{r_2}\right)}{\sqrt{\gamma_l}} e^{-jh_l Z}. \end{aligned}\right\} \quad (1)$$

$$\left.\begin{aligned} H_\theta^{\mathrm{I}} &= \frac{\omega\varepsilon}{h_1} a_1^i \frac{J_1\left(\lambda_1 \frac{r}{r_1}\right)}{\sqrt{\gamma_1}} e^{-jh_1 Z} - \sum_{l=1}^{\infty} \frac{\omega\varepsilon}{h_l} a_l \frac{J_1\left(\lambda_l \frac{r}{r_1}\right)}{\sqrt{\gamma_l}} e^{jh_l Z} \\ H_\theta^{\mathrm{II}} &= -\frac{\omega\varepsilon}{h_1} b_1^i \frac{J_1\left(\lambda_1 \frac{r}{r_1}\right)}{\sqrt{\gamma_1}} e^{jh_1 Z} + \sum_{l=1}^{\infty} \frac{\omega\varepsilon}{h_l} b_l \frac{J_1\left(\lambda_l \frac{r}{r_1}\right)}{\sqrt{\gamma_l}} e^{-jh_l Z}. \end{aligned}\right\} \quad (2)$$

But, in the above equations, indices, I, II mean region I, II respectively, and a_1^i, b_1^i,

mean the incident wave amplitudes from region I, II, a_l, b_l mean the excited l_{th} mode amplitudes caused by the junction part in the region I, II respectively, and h_l, $h_{\tilde{l}}$ are the propagation constants of the l_{th} modes along its axis and they are represented in the following equations.

$$h_l^2 = K^2 - \left(\frac{\lambda_l}{r_1}\right)^2, \quad h_{\tilde{l}}^2 = K^2 - \left(\frac{\lambda_l}{r_2}\right)^2 \tag{3}$$

where $K=\omega\sqrt{\mu\varepsilon}$ means the propagation constant in free space and ε, μ are the medium constants of space and λ_l is the value of l_{th} zero of Bessel function of order zero. And γ_l, $\gamma_{\tilde{l}}$ are represented in the following equations.

$$\left.\begin{aligned} \gamma_l &= \int_0^{r_1} J_1\left(\lambda_l \frac{r}{r_1}\right)^2 r dr = \frac{1}{2} r_1^2 J_1(\lambda_l)^2 \\ \gamma_{\tilde{l}} &= \int_0^{r_1} J_1\left(\lambda_l \frac{r}{r_2}\right)^2 r dr = \frac{1}{2} r_2^2 J_1(\lambda_l)^2 . \end{aligned}\right\} \tag{4}$$

Now let us put the electric fields at the junction plane

$$E_r\Big|_{z=0} = \frac{\Psi(r)}{2} .$$

Then each coefficient of Eq. (1) is represented as follows by using the function $\Psi(r)$ and the orthogonal nature of Bessel functions.

$$\left.\begin{aligned} a_1^i + a_1 &= \int_0^{r_1} \Psi(r) \frac{J_1\left(\lambda_1 \frac{r}{r_1}\right)}{\sqrt{\gamma_1}} dr \\ a_l &= \int_0^{r_1} \Psi(r) \frac{J_1\left(\lambda_l \frac{r}{r_1}\right)}{\sqrt{\gamma_l}} dr \end{aligned}\right\} \tag{5}$$

$$\left.\begin{aligned} b_1^i + b_1 &= \int_0^{r_1} \Psi(r) \frac{J_1\left(\lambda_1 \frac{r}{r_2}\right)}{\sqrt{\gamma_l}} dr \\ b_l &= \int_0^{r_1} \Psi(r) \frac{J_1\left(\lambda_l \frac{r}{r_2}\right)}{\sqrt{\gamma_l}} dr . \end{aligned}\right\} \tag{6}$$

Next, substituting these coefficients into Eq. (2) and using the condition of continuity of H_θ at the junction plane, following integral equation is obtained.

$$f(r) + \int_0^{r_1} \Psi(r') G(r, r') dr' = 0 \tag{7}*$$

---

* The direct solving of Eq. (7) takes the considerable trouble and result obtained by this is not convenient form for later calculation.

where

$$\left.\begin{aligned} f(r) &= -2\left[\frac{b_1^i}{h_1\tilde{\gamma}}\frac{J_1\left(\lambda_1\frac{r}{r_2}\right)}{\sqrt{\tilde{\gamma}_1}}+\frac{a_1^i}{h_1}\frac{J_1\left(\lambda_1\frac{r}{r_1}\right)}{\sqrt{\tilde{\gamma}_1}}\right] \\ G(r,\ r') &= \sum_{l=1}^{\infty}\left[\frac{J_1\left(\lambda_l\frac{r}{r_1}\right)J_1\left(\lambda_l\frac{r'}{r_1}\right)}{h_l''_l}+\frac{J_1\left(\lambda_l\frac{r}{r_2}\right)J_1\left(\lambda_l\frac{r'}{r_2}\right)}{h_{\tilde{\gamma}}\tilde{\gamma}_{\tilde{\gamma}}}\right]. \end{aligned}\right\} \tag{8}$$

Multiplying the both sides of Eq. (7) by $\Psi(r)$ and integrating over r from 0 to r_1, the following second order form of the integral equation is obtained.

$$\int_0^{r_1} f(r)\Psi(r)dr+\int_0^{r_1}\int_0^{r_1}\Psi(r)G(r,\ r')\Psi(r')drdr'=0. \tag{9}$$

By this treatment, if the form of the function of r, $\Psi(r)$ is set so as to satisfy the boundary condition of junction plane, its unknown coefficient is determined by using Eq. (9).

In order to choose the form of function r, $\Psi(r)$, we take the following nature that $E(r)$ is zero at $r=0$, ∞ at $r=r_1$, into consideration and it is possible to integrate over the domain which include this singularity.

We have

$$\begin{aligned} \Psi(r) &= \frac{Ar^2}{\sqrt{r_1^2-r^2}} \quad \cdots\cdots \quad 0\leqq r\leqq r_1 \\ &= 0 \qquad\qquad \cdots\cdots \quad r_1\leqq r\leqq r_2 \end{aligned} \tag{10}$$

where A is an unknown coefficient.

And to carry out the calculation, we set up the following representation.

$$\begin{aligned} &\int_0^{r_1}\frac{r^2}{\sqrt{r_1^2-r^2}}J_1\left(\lambda_l\frac{r}{r_1}\right)dr = r_1^2\sqrt{\frac{\pi}{2\lambda_l}}J_{\frac{3}{2}}(\lambda_l) = r_1^2 j_1(\lambda_l)\equiv\alpha_l \\ &\int_0^{r_1}\frac{r^2}{\sqrt{r_1^2-r^2}}J_1\left(\lambda_l\frac{r}{r_2}\right)dr = r_1^2\sqrt{\frac{\pi}{2\lambda_l\frac{r_1}{r_2}}}J_{\frac{3}{2}}\left(\lambda_l\frac{r_1}{r_2}\right) = r_1^2 j_1\left(\lambda_l\frac{r_1}{r_2}\right)\equiv\beta_l \ * \\ &j_1(x) = \frac{\sin x}{x^2}-\frac{\cos x}{x}. \end{aligned} \tag{11}$$

Now we will try to solve the integral equation of (7) in the following two cases.

Case I, Incident wave is excited from the region I.

In this case b_1^i in Eq. (8) should be zero, then the unknown coefficient A is determined from Eq. (9) and its result is as follows.

$$A = \frac{\frac{2\alpha_1}{\sqrt{\tilde{\gamma}_1}h_1}a_1^i}{\sum_{l=1}^{\infty}\left[\frac{\alpha_l^2}{h_l''_l}+\frac{\beta_l^2}{h_{\tilde{\gamma}}\tilde{\gamma}_{\tilde{\gamma}}}\right]}. \tag{12}$$

* The formula of Sonine's 1st integral is used to obtain these relations.

Then from Eq. (5) the next equation is obtained.

$$a_1 = \frac{2a_1^i\alpha_1^2}{h_1\gamma_1\sum_{l=1}^{\infty}\left[\frac{\alpha_l^2}{h_l\gamma_l}+\frac{\beta_l^2}{h_{\tilde{l}}\gamma_{\tilde{l}}}\right]} - a_1^i . \tag{13}$$

If the notation Γ represents the reflection coefficient, then we can rewrite as follows.

$$\Gamma = \frac{a_1}{a_1^i} = \frac{2\alpha_1^2}{h_1\gamma_1\sum_{l=1}^{\infty}\left[\frac{\alpha_l^2}{h_l\gamma_l}+\frac{\beta_l^2}{h_{\tilde{l}}\gamma_{\tilde{l}}}\right]} - 1 . \tag{14}$$

Accordingly the normalized admittance Y_0 looking into right side through the junction part is represented the following equation by using Γ.

$$Y_0 = \frac{1-\Gamma}{1+\Gamma} = \frac{\gamma_1\beta_1^2}{\gamma_{\tilde{1}}\alpha_1^2}\left[\frac{h_1}{h_{\tilde{1}}}+\frac{\gamma_{\tilde{1}}h_1}{\beta_1^2}\sum_{l=2}^{\infty}\left\{\frac{\alpha_l^2}{h_l\gamma_l}+\frac{\beta_l^2}{h_{\tilde{l}}\gamma_{\tilde{l}}}\right\}\right]. \tag{15}$$

And considering that the characteristic admittance of each guide in this case is represented by $Y_1=\frac{\omega\varepsilon}{h_1}$, $Y_2=\frac{\omega\varepsilon}{h_{\tilde{1}}}$ respectively, Eq. (15) is rewritten as Eq. (16)

$$Y_0 = \frac{1}{n^2}\left[\frac{Y_2}{Y_1}+j\frac{B}{Y_1}\right], \tag{16}$$

where

$$n = \frac{r_2 j_1(\lambda_1)}{r_1 j_1\left(\lambda\frac{r_1}{r_2}\right)}$$

$$B = \omega\varepsilon\left[\frac{J_1(\lambda_1)}{\frac{r_1}{r_2}j_1\left(\lambda_1\frac{r_1}{r_2}\right)}\right]^2\sum_{l=2}^{\infty}\left[\frac{1}{h_l'}\left\{\frac{j_1(\lambda_l)}{J_1(\lambda_l)}\right\}^2+\frac{1}{h_{\tilde{l}}'}\left\{\frac{\frac{r_1}{r_2}j_1\left(\lambda_l\frac{r_1}{r_2}\right)}{J_1(\lambda_l)}\right\}^2\right]$$

h_l', $h_{\tilde{l}}'$ $[l>1]$ are positive numbers and

$h_l' = jh_l$, $h_{\tilde{l}}' = jh_{\tilde{l}}$.

The series in B converges.

Case II, Incident wave is excited from the region II.

In this case, a_1^i in Eq. (8) should be zero, then this result agrees with the equivalent circuit representation obtained in the previous section.

1.3 The case in which H_{01} mod is propagated.

The same assumption used in 1.2, is taken place in this case too. And the characteristics of the junction part are obtained from the condition of continuity of E_θ, H_r.

When the incident wave H_{01} is propagated from either one of the two guides, the transverse field components of both sides of the junction part are represented as follows.

$$\left.\begin{aligned} E_\theta^{\mathrm{I}} &= a_1^i \frac{J_1\left(\lambda_1 \frac{r}{r_1}\right)}{\sqrt{\gamma_1}} e^{-jh_1 z} + \sum_{l=1}^{\infty} a_l \frac{J_1\left(\lambda_l \frac{r}{r_1}\right)}{\sqrt{\gamma_l}} e^{jh_l z} \\ E_\theta^{\mathrm{II}} &= b_1^i \frac{J_1\left(\lambda_1 \frac{r}{r_2}\right)}{\sqrt{\gamma_1 \tilde{\gamma}}} e^{jh_1 z} + \sum_{l=1}^{\infty} b_l \frac{J_1\left(\lambda_l \frac{r}{r_2}\right)}{\sqrt{\gamma_l \tilde{\gamma}}} e^{-jh_{\tilde{l}} z}. \end{aligned}\right\} \tag{17}$$

$$\left.\begin{aligned} H_r^{\mathrm{I}} &= -a_1^i \frac{h_1}{\omega\mu} \frac{J_1\left(\lambda_1 \frac{r}{r_1}\right)}{\sqrt{\gamma_1}} e^{-jh_1 z} + \sum_{l=1}^{\infty} a_l \frac{h_l}{\omega\mu} \frac{J_1\left(\lambda_l \frac{r}{r_1}\right)}{\sqrt{\gamma_l}} e^{jh_l z} \\ H_r^{\mathrm{II}} &= b_1^i \frac{h_{\tilde{1}}}{\omega\mu} \frac{J_1\left(\lambda_1 \frac{r}{r_2}\right)}{\sqrt{\gamma_1 \tilde{\gamma}}} e^{jh_{\tilde{1}} z} - \sum_{l=1}^{\infty} b_l \frac{h_{\tilde{l}}}{\omega\mu} \frac{J_1\left(\lambda_l \frac{r}{r_2}\right)}{\sqrt{\gamma_l \tilde{\gamma}}} e^{-jh_{\tilde{l}} z}, \end{aligned}\right\} \tag{18}$$

where λ_l is the value of l th zero of the Besel function of the 1st order, and results in this case are

$$\gamma_l = \frac{r_1^2}{2} J_0(\lambda_l)^2, \quad \gamma_{\tilde{l}} = \frac{r_2^2}{2} J_0(\lambda_l)^2$$

and the other notations are same as is used in case 1. 2.

Similarly, representing the coefficients of Eq. (17) by $\Psi(r)$ which depends upon the electric field of the junction plane and substituting them into the equation of continuity of H_r, then we obtain the following integral equation.

$$f(r) + \int_0^{r_1} \Psi(r') G(r, r') dr' = 0 \tag{19}$$

where

$$f(r) = -2\left[a_1^i h_1 \frac{J_1\left(\lambda_1 \frac{r}{r_1}\right)}{\sqrt{\gamma_1}} + b_1^i h_{\tilde{1}} \frac{J_1\left(\lambda_1 \frac{r}{r_2}\right)}{\sqrt{\gamma_1 \tilde{\gamma}}}\right]$$

$$G(r, r') = \sum_{l=1}^{\infty}\left[\frac{h_l}{\gamma_l} J_1\left(\lambda_l \frac{r}{r_1}\right) J_1\left(\lambda_l \frac{r'}{r_1}\right) + \frac{h_{\tilde{l}}}{\gamma_l \tilde{\gamma}} J_1\left(\lambda_l \frac{r}{r_2}\right) J_1\left(\lambda_l \frac{r'}{r_2}\right)\right].$$

To solve this equation, again we transform this into the integral equation of the second order and set the form of $\Psi(r)$ to satisfy its boundary condition, namely

$$\left.\begin{aligned} \Psi(r) &= Ar^2(r_1^2 - r^2) \qquad 0 \leqq r \leqq r_1 \\ &= 0 \qquad\qquad\qquad r_1 \leqq r \leqq r_2 \end{aligned}\right\} \tag{20}$$

Then the normalized admittance Y_0 looking into the right side through the junction plane is obtained the following equation by the similar calculations.

$$Y_0 = \frac{1}{n^2}\left[\frac{Y_2}{Y_1} - \frac{jB}{Y_1}\right], \tag{21}$$

where

$$n = \frac{r_1 J_3(\lambda_1)}{r_2 J_3\left(\lambda_1 \frac{r_1}{r_2}\right)}$$

$$B = \frac{\lambda_1^4 r_1^2 J_0(\lambda_1)^2}{\omega\mu r_2^2 J_3\left(\lambda_1 \frac{r_1}{r_2}\right)} \sum_{l=2}^{\infty} \left[\frac{h_l' J_3(\lambda_l)^2}{\lambda_l^4 J_0(\lambda_l)^2} + \frac{h_l'' J_3\left(\lambda_l \frac{r_1}{r_2}\right)^2}{\lambda_l^4 \frac{r_1^2}{r_2^2} J_0(\lambda_l)^2} \right],$$

$Y_1 = \frac{h_1}{\omega\mu}$, $Y_2 = \frac{h_1''}{\omega\mu}$: the characteristic admittance of each guide in this case.

Physical explanation of Eq. (16) or Eq. (21) is shown in Fig. 1.2 as the equivalent circuit representation. This means that the higher modes which satisfy the boundary condition of junction part of wave guides in each case behaves as shunt admittance Y and this seems to be bridge across an ideal transformer, turn ratio of which is function of the ratio of radii of the two waveguides jointed. Y is capacitive in case which E_{01} wave propagated and is inductive in case of H_{01} wave.

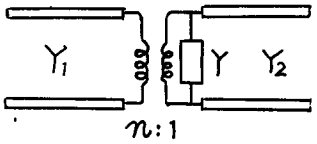

Fig. 1.2. Equivalent circuit representation.

1.4 The Utilization of Variational Method.

The determination of the form of function of $\Psi(r)$ described in the previous sections are performed from the two stand points; it satisfies the boundary condition of jnction plane and it is possible to integrate over the domain with its singularity. Therefore such $\Psi(r)$ does not yet represent the rigorous solution. So in order to get the rigorous solution, the linear combinations of more trial functions each of which satisfies the two conditions mentioned above are necessary, and the determination of that coefficients is performed by the variational method.[2]

However, for the practical use, the treatments of previous sections are considered to be sufficient, so that the concrete calculations using the variational method are not treated here.

Chapter 2. The Characteristics of Some Cylindrical Substances in a Rectangular Wave Guide.

2.1 Introduction

In this Chapter, an attempt to analyse strictly the problem how cylindrical substances act in a rectangular wave guide is made.

Analyses are performed in the case of the cylindrical substances inserted in parallel with the primary electric field in the wave guide by using both Cartesian and Cylindrical coordinate systems. And the method of the image principle[3] is used for the calculation with the assumption that the inserted substances and the wave guide have no losses.

2.2 The Case of a Circular Hollow Dielectric Post inserted into a Rectangular Wave Guide.

When the primary field is excited in the wave guide which has an dielectric post inside of it as shown in Fig. 2.1, its field is disturbed by the dielectric post and perturbed field is arised. But in the case of the diameter of the dielectric post is invariable along Z direction such as Fig. 2.1, the perturbed field has the electric fields component only along Z direction.

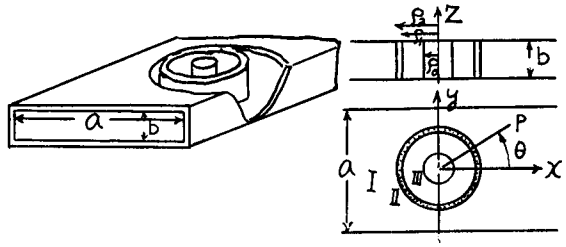

Fig. 2.1. The configuration of a circular hollow dielectric post in the rectangular wave guide.

The process of the analysis is as follows; first, the primary field in the wave guide which is usually expressed by a cartesian coordinate system is expanded into the cylindrical elemental waves expressed by a cylindrical coordinate, axis of which is placed on that of the post, second, the perturbed field is represented by the superposition of the resultant fields of the cylindrical elemental waves arised by the post and their images, and these amplitudes are so decided as to satisfy the boundary condition on the post wall.

The wave guide region is divided into the following three parts. Part I is the region outside the post, Part II is the region of the dielectrics and Part III is the region inside the post.

The dielectric constant, permeability and propagation constant of each region are denoted by ε_1, μ_1, κ_1, ε_2, μ_2, κ_2 and ε_1, μ_1, κ_1, respectively. And among them there are following relations

$$\kappa_1 = \omega\sqrt{\varepsilon_1\mu_1}, \quad \kappa_2 = \omega\sqrt{\varepsilon_2\mu_2},$$

where ω is a angular frequency. Besides, the relation $\mu_1 \simeq \mu_2$ is satisfied, if the dielectrics have no ferromagnetic properties.

Then let us represent the primary field as the following form by omitting its time factor $e^{j\omega t}$.

$$E_{\text{prim}} = E_Z = e^{-jL_1 x}\cos\alpha_1 y. \tag{1}$$

Representing Eq. (1) by the cylindrical coordinate system, we obtain the following expression

$$E_{\text{prim}} = \sum_{n=0}^{\infty} e_n J_n(\kappa_1 r)\cos n\theta, \tag{2}$$

where
$$e_0 = 1, \quad e_{2n} = 2\cos 2n\Psi, \quad \cdots\cdots \quad n = 1, 2, \cdots\cdots$$
$$e_{2n+1} = -2j\sin(2h+1)\Psi, \quad \cdots\cdots \quad n = 0, 1, \cdots\cdots$$

and

$$L_1 = \sqrt{\kappa_1^2 - \alpha_1^2}, \quad \alpha_1 = \frac{\Pi}{a}, \quad \Psi = \sin^{-1}\frac{L_1}{K_1}.$$

The perturbed field arised by the post is represented by the form $\sum_{n=0}^{\infty} A_n \kappa_1^2 H_n^{(2)}(\kappa_1 r) \times \cos n\theta$ in the case that the wave guide has not side walls. But by considering the image sources of the perturbed field we can represent the perturbed field in the case of when sidewalls are placed. Calculating it on this principle we obtain the following results.

$$\sum_{n=0}^{\infty} A_n \kappa_1^2 H_n^{(2)}(\kappa_1 r)\cos n\theta + 2\sum_{n=0}^{\infty}\sum_{\nu=-\infty}^{+\infty} A_n \kappa_1^2 H_{n+\nu}^{(\tilde{2})}(\kappa_1 a) J_\nu(\kappa_1 r) \times \cos\frac{(n-\nu)\pi}{2}\cos n\theta, \tag{3}$$

where

$$H_n^{(\tilde{2})}(Z) = \sum_{P=1}^{\infty}(-)^P H_n^{(2)}(PZ).$$

In the above equations we considered only electric fields in region I, hence E_Z, H_θ components of each regions are described as follows.

region I.

$$\left.\begin{aligned} E_Z^{\mathrm{I}} &= E_{\text{prim.}} + E_{Z\,\text{pert.}} = \sum_{n=0}^{\infty} e_n J_n(\kappa_1 r)\cos n\theta + \kappa_1^2 \sum_{n=0}^{\infty} A_n H_n^{(2)}(\kappa_1 r)\cos n\theta \\ &\quad + 2\kappa_1^2 \sum_{n=0}^{\infty}\sum_{\nu=-\infty}^{+\infty} A_n H_{n+\nu}^{(\tilde{2})}(\kappa_1 a) J_\nu(\kappa_1 r)\cos\frac{(n-\nu)\pi}{2}\cos n\theta \\ H_\theta^{\mathrm{I}} &= H_{\theta\,\text{prim.}} + H_{\theta\,\text{pert.}} = \frac{1}{j\mu_1\omega}\sum_{n=0}^{\infty} e_n J_n'(\kappa_1 r)\cos n\theta - j\omega\varepsilon_1 \sum_{n=0}^{\infty} A_n H_n^{(2)\prime}(\kappa_1 r)\cos n\theta \\ &\quad - 2j\omega\varepsilon_1 \sum_{n=0}^{\infty}\sum_{\nu=-\infty}^{+\infty} A_n H_{n+\nu}^{(\tilde{2})}(\kappa_1 a) J_\nu'(\kappa_1 r)\cos\frac{(n-\nu)\pi}{2}\cos n\theta \end{aligned}\right\} \tag{4}$$

region II.

$$\left.\begin{aligned} E_Z^{\mathrm{II}} &= \kappa_2^2 \sum_{n=0}^{\infty}\{B_n J_n(\kappa_2 r) + C_n Y_n(\kappa_2 r)\}\cos n\theta \\ H_\theta^{\mathrm{II}} &= -j\omega\varepsilon_2 \sum_{n=0}^{\infty}\{B_n J_n'(\kappa_2 r) + C_n Y_n'(\kappa_2 r)\}\cos n\theta \end{aligned}\right\} \tag{5}$$

rigion III.

$$\left.\begin{aligned} E_Z^{\mathrm{III}} &= \kappa_1^2 \sum_{n=0}^{\infty} D_n J_n(\kappa_1 r)\cos n\theta \\ H_\theta^{\mathrm{III}} &= -j\omega\varepsilon_1 \sum_{n=0}^{\infty} D_n J_n'(\kappa_1 r)\cos n\theta, \end{aligned}\right\} \tag{6}$$

where A_n, B_n, C_n and D_n are the unknown coefficients, and the prime, means the derivative with respect to r of the argument here.

Now, since the tangential components of the electromagnetic fields in the adjacent

regions are equal to each other on the boundary surfaces ρ_1, ρ_2 comparing the coefficients of $\cos n\theta$, we obtain the following simultaneous equations about the unknown coefficients.

$$\left.\begin{aligned} e_n J_n(\kappa_1\rho_2)+A_n\kappa_1^2\alpha_n-B_n\kappa_2^2 J_n(\kappa_2\rho_2)-C_n\kappa_2^2 Y_n(\kappa_2\rho_2) &= 0\\ B_n\kappa_2^2 J_n(\kappa_2\rho_1)+C_n\kappa_2^2 Y_n(\kappa_2\rho_1)-D_n\kappa_1^2 J_n(\kappa_1\rho_2) &= 0\\ e_n J_n'(\kappa_1\rho_2)+A_n\kappa_1^2\beta_n-B_n\kappa_2^2 J_n'(\kappa_2\rho_2)-C_n\kappa_2^2 Y_n'(\kappa_2\rho_2) &= 0\\ B_n\kappa_2^2 J_n'(\kappa_2\rho_1)+C_n\kappa_2^2 Y_n'(\kappa_2\rho_1)-D_n\kappa_1^2 J_n'(\kappa_1\rho_2) &= 0, \end{aligned}\right\} \quad (7)$$

where

$$\left.\begin{aligned} \alpha_n &= H_n^{(2)}(\kappa_1\rho_2)+\Delta_n 2H_{2n}^{(\tilde{2})}(\kappa_1 a)J_n(\kappa_1\rho_2)+2H_0^{(\tilde{2})}(\kappa_1 a)J_n(\kappa_1\rho_2)\\ \beta_n &= H_n^{(2)\prime}(\kappa_1\rho_2)+\Delta_n 2H_{2n}^{(\tilde{2})}(\kappa_1 a)J_n'(\kappa_1\rho_2)+2H_0^{(\tilde{2})}(\kappa_1 a)J_n'(\kappa_1\rho_2) \end{aligned}\right\} \quad (8)$$

$$\Delta_n = 0 \quad \cdots\cdots \quad n=0$$
$$= 1 \quad \cdots\cdots \quad n>0.$$

By solving Eq. (7), we determine the unknown coefficients, which represent the fields. But among these coefficients, only A_n is wanted in order to reduce the equivalent circuit of the post, as is described in the following.

We obtain A_n as follows by method of determinant.

$$A_n = \frac{-e_n\{J_n(\kappa_1\rho_1)\cdot X+J_n'(\kappa_1\rho_2)\cdot Y\}}{\kappa_1^2(\alpha_n\cdot X+\beta_n\cdot Y)}, \quad (9)$$

where

$$\begin{aligned} X = \{&J_n'(\kappa_1\rho_1)J_n(\kappa_2\rho_1)Y_n'(\kappa_2\rho_2)+J_n(\kappa_1\rho_1)J_n'(\kappa_2\rho_2)Y_n'(\kappa_2\rho_1)\\ &-J_n(\kappa_1\rho_1)J_n'(\kappa_2\rho_1)Y_n'(\kappa_2\rho_2)-J_n'(\kappa_1\rho_1)J_n'(\kappa_2\rho_2)Y_n(\kappa_2\rho_1)\}\\ Y = \{&J_n(\kappa_1\rho_1)J_n'(\kappa_2\rho_1)Y_n(\kappa_2\rho_2)+J_n'(\kappa_1\rho_1)J_n(\kappa_2\rho_2)Y_n(\kappa_2\rho_1)\\ &-J_n'(\kappa_1\rho_1)J_n(\kappa_2\rho_1)Y_n(\kappa_2\rho_2)-J_n(\kappa_1\rho_1)J_n(\kappa_2\rho_2)Y_n'(\kappa_2\rho_1)\}. \end{aligned}$$

Separating the real parts of α_n, β_n from imaginary part of them, we rewrite A_n as follows.

$$A_n = \frac{-e_n}{\kappa_1^2} \times \frac{1}{\left[1+\Delta_n 2J_{\tilde{2}n}(\kappa_1 a)+2J_{\tilde{0}}(\kappa_1 a)-j\left\{\dfrac{M_n Y_n(\kappa_1\rho_2)-Y_n'(\kappa_1\rho_2)}{M_n J_n(\kappa_1\rho_2)-J_n'(\kappa_1\rho_2)+\Delta_n 2Y_{\tilde{2}n}(\kappa_1 a)+2Y_{\tilde{0}}(\kappa_1 a)}\right\}\right]}, \quad (10)$$

where

$$M_n = -\frac{X}{Y} = \frac{J_n(\kappa_1\rho_1)[J_n'(\kappa_2\rho_1)Y_n'(\kappa_2\rho_2)-J_n'(\kappa_2\rho_2)Y_n'(\kappa_2\rho_1)]}{J_n(\kappa_1\rho_1)[J_n'(\kappa_2\rho_1)Y_n(\kappa_2\rho_2)-J_n(\kappa_2\rho_2)Y_n'(\kappa_2\rho_1)]} \frac{-J_n'(\kappa_1\rho_1)[J_n(\kappa_2\rho_1)Y_n'(\kappa_2\rho_2)-J_n'(\kappa_2\rho_2)Y_n(\kappa_2\rho_1)]}{-J_n'(\kappa_1\rho_1)[J_n(\kappa_2\rho_1)Y_n(\kappa_2\rho_2)-J_n(\kappa_2\rho_2)Y_n(\kappa_2\rho_1)]}. \quad (11)$$

In the case of $\kappa_1\rho_2<1$, the perturbed field can be represented sufficiently only by A_0 and A_1. Then they become

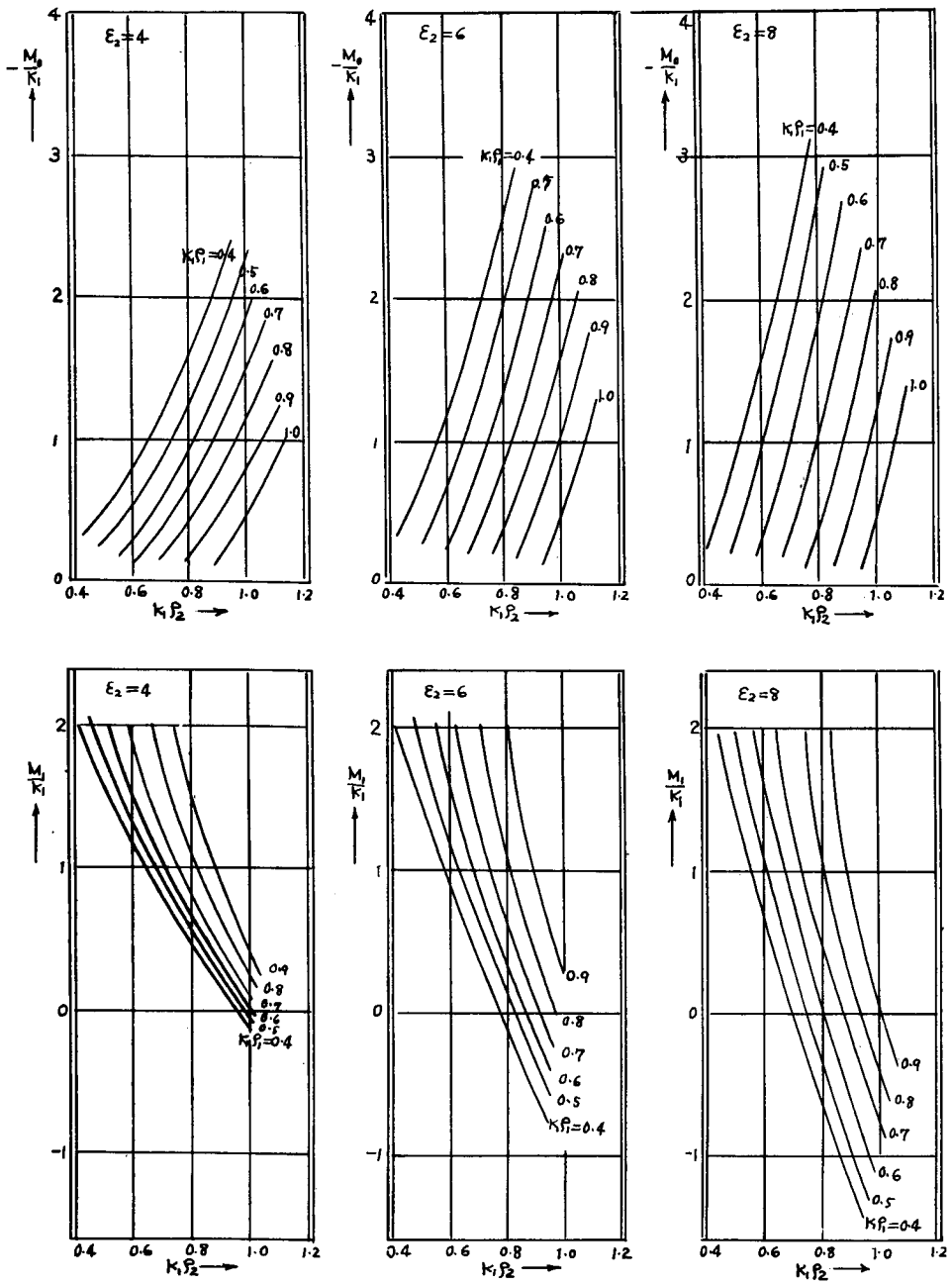

Fig. 2.2. The graphical representation of the relations between M_0/κ_1, M_1/κ_1 and $\kappa_1\rho_2$ parameter of which is $\kappa_1\rho_1$.

$$A_0 = -\frac{1}{\kappa_2^1}\left[\frac{1}{\{1+2J_{\tilde{0}}(\kappa_1 a)\}+j\left\{\dfrac{\dfrac{M_0}{\kappa_1}Y_0(\kappa_1\rho_2)+Y_1(\kappa_1\rho_2)}{\dfrac{M_0}{\kappa_1}J_0(\kappa_1\rho_2)+J_1(\kappa_1\rho_2)}+2Y_{\tilde{0}}(\kappa_1 a)\right\}}\right] \tag{12}$$

$$A_1=\frac{2j\sin\Psi}{\kappa_1^2}$$

$$\times\left[\frac{1}{\{1+2J_{\tilde{2}}(\kappa_1 a)\}+2J_{\tilde{0}}(\kappa_1 a)\}-j\left\{\dfrac{\left(\dfrac{M_0}{\kappa_1}+\dfrac{1}{\kappa_1\rho_2}\right)Y_1(\kappa_1\rho_2)-Y_0(\kappa_1\rho_2)}{\left(\dfrac{M_0}{\kappa_1}+\dfrac{1}{\kappa_1\rho_2}\right)J_1(\kappa_1\rho_2)-J_0(\kappa_1\rho_2)+2Y_{\tilde{2}}(\kappa_1 a)+2Y_{\tilde{0}}(\kappa_1 a)}\right\}}\right]. \tag{13}$$

In the above equations, $\frac{M_0}{\kappa_1}$, $\frac{M_1}{\kappa_1}$ are represented by the following equations.

$$\frac{M_0}{\kappa_1}=\frac{J_1(\kappa_1\rho_1)Z_{0\cdot1}(1\cdot2)-\frac{\kappa_2}{\kappa_1}J_0(\kappa_1\rho_1)Z_{1\cdot1}(1\cdot2)}{J_0(\kappa_1\rho_1)Z_{1\cdot0}(1\cdot2)-\frac{\kappa_1}{\kappa_2}J_1(\kappa_1\rho_1)Z_{0\cdot0}(1\cdot2)} \tag{14}$$

$$\frac{M_1}{\kappa_1}=\frac{\frac{\kappa_2}{\kappa_1}J_1(\kappa_1\rho_1)\left[Z_{0\cdot0}(1\cdot2)-\frac{1}{\kappa_2\rho_2}Z_{0\cdot1}(1\cdot2)\right]-J_0(\kappa_1\rho_1)\left[Z_{1\cdot0}(1\cdot2)-\frac{1}{\kappa_2\rho_2}Z_{1\cdot1}(1\cdot2)\right]}{J_1(\kappa_1\rho_1)Z_{0\cdot1}(1\cdot2)-\frac{\kappa_1}{\kappa_2}J_0(\kappa_1\rho_1)Z_{1\cdot1}(1\cdot2)}, \tag{15}$$

where

$$Z_{p\cdot q}(1\cdot2)\equiv J_p(\kappa_2\rho_1)Y_q(\kappa_2\rho_2)-Y_p(\kappa_2\rho_1)J_q(\kappa_2\rho_2)$$
$$(p\cdot q=0,\ \text{or}\ 1). \tag{16}$$

In the above Eq. (14), (15), M_0/κ_1, M_1/κ_1 seem to be very complicated, but being expressed in an generalized form as the function of κ_2/κ_1, $\kappa_1\rho_1$, $\kappa_1\rho_2$ is applicable for any case. Fig. 2.2 shows the relation among M_0/κ_1, M_1/κ_1, $\kappa_1\rho_1$ and $\kappa_1\rho_2$ in the cases $\varepsilon_2=4$, 6, 8.

Now in order to obtain the equivalent circuit, we must get the reflection und transmission coefficients of the incident wave. These are represented as follows considering the limiting values of $x\to-\infty$ and $+\infty$ of the electromagnetic fields after the transformation from the cylindrical coordinate into the cartesian.

$$R=\frac{4\kappa_1^2}{L_1 a}\left\{\sum_{n=0}^{\infty}A_{2n}\cos 2n\Psi-j\sum_{n=0}^{\infty}A_{2n+1}\sin(2n+1)\Psi\right\} \tag{17}^{3)}$$

$$T=1+\frac{4\kappa_1^2}{L_1 a}\left\{\sum_{n=0}^{\infty}A_{2n}\cos 2n\Psi+j\sum_{n=0}^{\infty}A_{2n+1}\sin(2n+1)\Psi\right\}. \tag{18}$$

Substituting the relations of Eq. (12), (13) to the above equations, we obtain R and T.

While, an equivalent symmetrical T network the reference plane of which is placed on the centre line of symmetry, as shown in Fig. 2.3 is obtained by solving the equations of the networks represented by R and T.

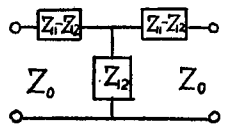

Fig. 2.3. Equivalent T type network.

The equivalent circuit elements obtained are as follows.

$$\left.\begin{aligned} Z_{11} &= j\left(\frac{M}{2}-\frac{1}{2N}\right)Z_0 \\ Z_{12} &= j\left(\frac{M}{2}+\frac{1}{2N}\right)Z_0 \\ Z_{11}-Z_{12} &= -j\left(\frac{1}{N}\right)Z_0\,, \end{aligned}\right\} \tag{19}$$

where

$$M = -\frac{\pi a}{2\lambda_g}\left\{\frac{\frac{M_0}{\kappa_1}Y_0(\kappa_1\rho_2)+Y_1(\kappa_1\rho_2)}{\frac{M_0}{\kappa_1}J_0(\kappa_1\rho_2)+J_1(\kappa_1\rho_2)}+2Y_{\tilde{0}}(\kappa_1)\right\} \tag{20}$$

$$N = -\frac{\pi\lambda_g a}{4\lambda^2}\left\{\frac{\left(\frac{M_1}{\kappa_1}+\frac{1}{\kappa_1\rho_2}\right)Y_1(\kappa_1\rho_2)-Y_0(\kappa_1\rho_2)}{\left(\frac{M_1}{\kappa_1}+\frac{1}{\kappa_1\rho_2}\right)J_1(\kappa_1\rho_2)-J_0(\kappa_1\rho_2)}+2Y_{\tilde{2}}(\kappa_1 a)+2Y_{\tilde{0}}(\kappa_1 a)\right\} \tag{21}$$

Z_0; Characteristic impedance of the wave guide.

And the summation of the series $Y_{\tilde{0}}(\kappa_1 a)$ and $Y_{\tilde{2n}}(\kappa_1 a)$ in the equations were obtained by Goto[3]. Their graphical representation is shown in Fig. 2.4 in which the argument $\kappa_1 a$ is rewritten $q\pi$.

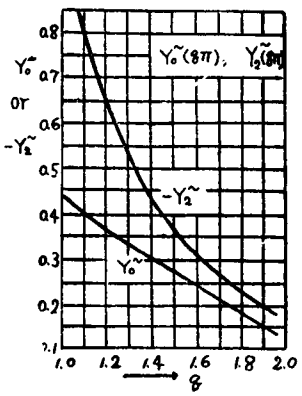

Fig. 2.4. The graphical representation of the relation between $Y_{\tilde{0}}$, $-Y_{\tilde{2}}$ and q.

Fig. 2.5 shows the frequency characteristics of the equivalent T network elements in the three cases of the different ε_2 of dielectric post ($\varepsilon_2=4, 6, 8$) whose outer radius is fixed to be 0.9 cm. and inner radius are varied in the rectangular wave guide of 5.8×2.9 cm. dimensions.

These results tell us the following tendency that the series element of the equivalent T network of the hollow dielectric post is inductive and the shunt element of it is capacitive and as the post thickness is increased, both elements tend to be inductive, this tendency, however, is brocken up when the value of ε_2 is increased and the sharp frequency characteristics come out.

2.3 The Case of a Metallic Post coxially surrounded by the Dielectric Cylinder inserted into the Wave-guide.

The configuration of the hollow dielectric cylinder and metallic post which are

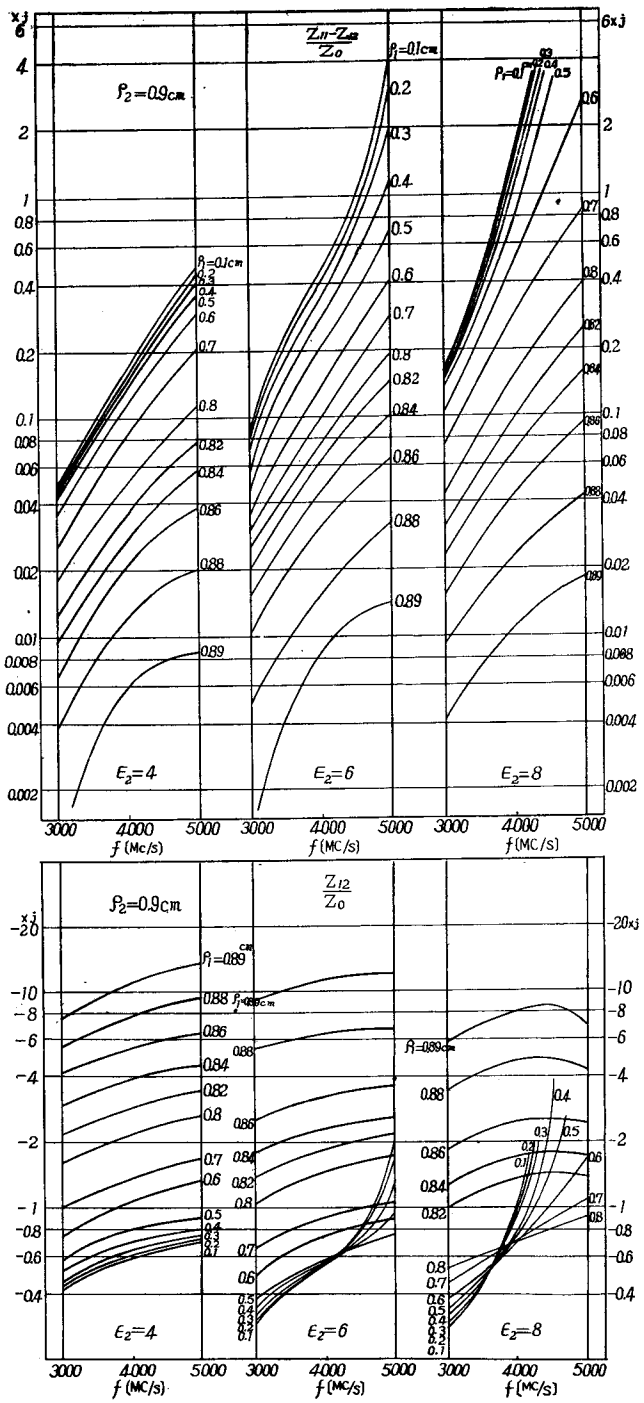

Fig. 2.5. Some characteristics of dielectric hollow cylinder in a rectangular wave guide.

inserted into the wave guide is shown in Fig. 2. 6.

In this case in the divided regions as shown in Fig. 2. 6, the forms of field components in the regions I, II are same as those of the preceding section, and in the region III the forms of field components are represented as follows.

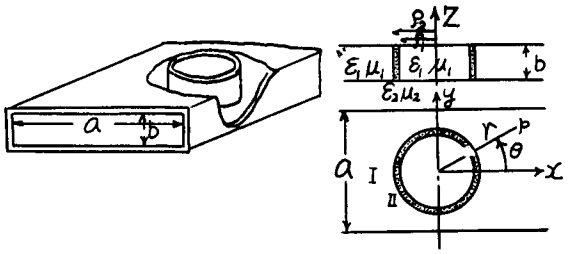

Fig. 2. 6. The configuration of the coaxial posts in a wave guide.

$$\left.\begin{aligned} E_Z^{\mathrm{III}} &= \kappa_1^2 \sum_{n=0}^{\infty} D_n \left[-\frac{Y_n(\kappa_1\rho_0)}{J_n(\kappa_1\rho_0)} J_n(\kappa_1 r) + Y_n(\kappa_1 r) \right] \cos n\theta \\ H_v^{\mathrm{III}} &= -j\omega\varepsilon_1 \sum_{n=0}^{\infty} D_n \left[-\frac{Y_n(\kappa_1\rho_0)}{J_n(\kappa_1\rho_0)} J_n'(\kappa_1 r) + Y_n'(\kappa_1 r) \right] \cos n\theta . \end{aligned}\right\} \tag{22}$$

By this correspondence, we obtain the values of the equivalent network of this case using the results of preceding section.

The values of M_0/κ_1, M_1/κ_1 in this case are as follows.

$$\frac{M_0}{\kappa_1} = \frac{C_{0\cdot1}(0\cdot1)Z_{0\cdot1}(1\cdot2) - \frac{\kappa_2}{\kappa_1} C_{0\cdot0}(0\cdot1)Z_{1\cdot1}(1\cdot2)}{C_{0\cdot0}(0\cdot1)Z_{1\cdot0}(1\cdot2) - \frac{\kappa_1}{\kappa_2} C_{0\cdot1}(0\cdot1)Z_{0\cdot0}(1\cdot2)} \tag{23}$$

$$\frac{M_1}{\kappa_1} = \frac{\frac{\kappa_2}{\kappa_1} C_{1\cdot1}(0\cdot1)\left[Z_{0\cdot0}(1\cdot2) - \frac{1}{\kappa_2\rho_2} Z_{0\cdot1}(1\cdot2) \right] - C_{1\cdot0}(0\cdot1)\left[Z_{1\cdot0}(1\cdot2) - \frac{1}{\kappa_2\rho_2} Z_{1\cdot1}(1\cdot2) \right]}{C_{1\cdot1}(0\cdot1)Z_{0\cdot1}(1\cdot2) - \frac{\kappa_1}{\kappa_2} C_{1\cdot0}(0\cdot1)Z_{1\cdot1}(1\cdot2)} , \tag{24}$$

where

$$\begin{aligned} C_{p\cdot q}(0\cdot1) &\equiv J_p(\kappa_1\rho_0)\, Y_q(\kappa_1\rho_1) - Y_p(\kappa_1\rho_0) J_q(\kappa_1\rho_1) \\ &\quad (p,\ q = 0 \text{ or } 1) . \end{aligned} \tag{25}$$

The results of calculation of the equivalent network by using the above equations represent the values of the precise equivalent T network of this case and these values include the mutual interference effect between the both.

Then their synthetic character is not the same as that of the network connections of the individual equivalent circuit of each post as shown in Fig. 2. 7 (where z_{mn}, Z_{mn} represent the values of dielectric post and metallic respectively) on account of the mutual interference effect. Fig. 2. 8 shows the numerical examples of the case when $\varepsilon_2 = 4$, $\rho_2 = 0.9$ cm, 0.86 cm and ρ_0 takes the several values.

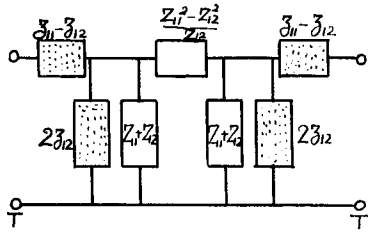

Fig. 2. 7. Equivalent network representation of the coaxial posts.

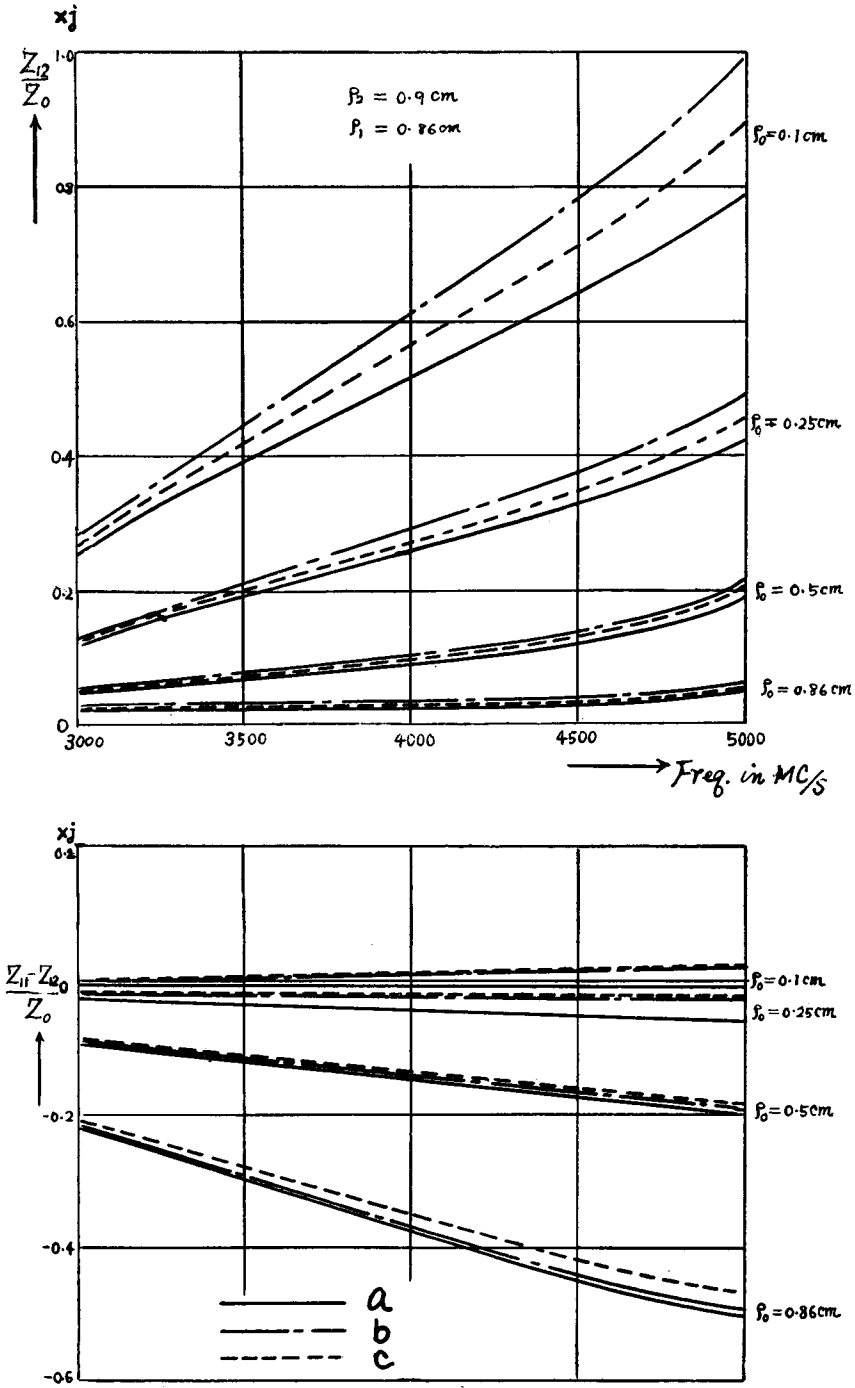

Fig. 2.8. Some characteristics of the metallic post coaxially surrounded by the dielectric cylinder inserted into the wave guide.

a: equivalent value of metallic post only.

b: the precise equivalent value of metallic post surrounded by dielectric cylinder.

c: network connection of the individual equivalent circuit of each post.

The equivalent circuit only metallic post inserted into the guide is calculated self-evidently by using the following M and N.

$$\left.\begin{aligned} M &= -\frac{\pi a}{2\lambda_g}\left[\frac{Y_0(\kappa_1\rho_0)}{J_0(\kappa_1\rho_0)} + 2Y_{\tilde{0}}(\kappa_1 a)\right] \\ N &= -\frac{\lambda_g a\pi}{4\lambda^2}\left[\frac{Y_1(\kappa_1\rho_0)}{J_1(\kappa_1\rho_0)} + 2Y_{\tilde{2}}(\kappa_1 a) + 2Y_{\tilde{0}}(\kappa_1 a)\right]. \end{aligned}\right\} \quad (26)^{3)}$$

We know from these calculations that the effect of the disturbance of the electromagnetic fields caused by thin hollow dielectric cylinder surrounding a metallic post becomes inductive.

Being the radius of the metallic post varied finely, the shunt elements of the dielectric post and the metallic resemble the antiresonance at a certain radius of a metallic post. In the neighborhood of this antiresonance the mutual interference of the both posts becomes dominant. And the mutual interference among the series elements becomes larger as the radius of metallic post approaches to the inner radius of a dielectric cylinder.

2.4 The Case of the Circular Metallic Post inserted partly into the Waveguide.

The configuration of this case is shown in Fig. 2.9.

The perturbed electromagnetic fields caused by the post can be represented as follows by using the electric and magnetic type Hertz vector potential, $\boldsymbol{U}$, $\boldsymbol{U}^*$.

$$\left.\begin{aligned} \boldsymbol{E} &= \nabla\times\nabla\times\boldsymbol{U} - j\omega\mu\nabla\times\boldsymbol{U}^* \\ \boldsymbol{H} &= j\varepsilon\omega\nabla\times\boldsymbol{U} + \nabla\times\nabla\times\boldsymbol{U}^*. \end{aligned}\right\} \quad (27)$$

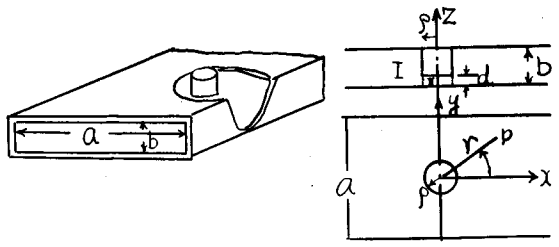

Fig. 2.9. The configuration of metallic post inserted into the wave guide.

When we assume that $\boldsymbol{U}$, $\boldsymbol{U}^*$ have the only Z component in the above equation, the components of the perturbed fields are represented as follows.

$$\left.\begin{aligned} E_r &= \frac{\partial^2 U}{\partial r\partial Z} - j\mu\omega\frac{1}{r}\frac{\partial U^*}{\partial\theta} & H_r &= j\varepsilon\omega\frac{1}{r}\frac{\partial U}{\partial\theta} + \frac{\partial^2 U^*}{\partial r\partial Z} \\ E_\vartheta &= \frac{1}{r}\frac{\partial^2 U}{\partial Z\partial\theta} + j\mu\omega\frac{\partial U^*}{\partial r} & H_\vartheta &= -j\varepsilon\omega\frac{\partial U}{\partial r} + \frac{1}{r}\frac{\partial^2 U^*}{\partial Z\partial\theta} \\ E_Z &= \kappa^2 U + \frac{\partial^2 U}{\partial Z^2} & H_Z &= \kappa^2 U^* + \frac{\partial^3 U^*}{\partial Z^3}. \end{aligned}\right\} \quad (28)$$

We divide the inner space of the guide into two regions, I. II and put the general solutions of U, U^* in each region as follows. (suffix I, II correspond to region I, II, respectively).

$$
\left.\begin{aligned}
U_{\mathrm{I}} &= \sum_{m=0}^{\infty}\sum_{n=0}^{\infty} A_{mn}H_n^{(2)}(\kappa_{rm}r)\cos n\theta\cos P_mZ \\
&\quad +2\sum_{m=0}^{\infty}\sum_{\nu=-\infty}^{+\infty}\sum_{n=0}^{\infty} A_{mn}H_{n+\nu}^{(\widetilde{2})}(\kappa_{rm}a)J_\nu(\kappa_{rm}r)\cos\frac{(n-\nu)\pi}{2}\cos\nu\theta\cos P_mZ^{**} \\
U_{\mathrm{II}} &= \sum_{m=0}^{\infty}\sum_{n=0}^{\infty} C_{mn}J_n(\kappa_{rm}'r)\cos n\theta\cos P_m'Z \\
U_{\mathrm{I}}^{*} &= \sum_{m=1}^{\infty}\sum_{n=1}^{\infty} B_{mn}H_n^{(2)}(\kappa_{rm}r)\sin n\theta\sin P_mZ \\
&\quad -2\sum_{m=1}^{\infty}\sum_{\nu=-\infty}^{\infty}\sum_{n=1}^{\infty} B_{mn}H_{n+\nu}^{(\widetilde{2})}(\kappa_{rm}a)J_\nu(\kappa_{rm}r)\cos\frac{(n-\nu)\pi}{2}\sin\nu\theta\sin P_mZ^{**} \\
U_{\mathrm{II}}^{*} &= \sum_{m=1}^{\infty}\sum_{n=1}^{\infty} D_{mn}J_n(\kappa'_{rm}r)\sin n\theta\sin P'_mZ\,,
\end{aligned}\right\} \qquad (29)
$$

where

$$
P_m = \frac{m\pi}{b} \qquad P_m' = \frac{m\pi}{d}
$$

$$
\kappa^2 - P_m^2 = \kappa_{rm}^2 \qquad \kappa^2 - P_m'^2 = \kappa_{rm}'^2
$$

$$
H_n^{(\widetilde{2})}(Z) = \sum_{P=1}^{\infty} H_n^{(2)}(PZ)\,.
$$

The functions with suffix I in the above equations satisfy the boundary conditions on the upper and lower planes and also the both side planes in the region I and the functions with suffix II satisfy the boundary ccnditions on the upper and lower planes in the region II.

The unknown coefficients in the above equations are so determined that the resultant field components of $E_Z\,E_\theta$, $H_Z\,H_\theta$ of one region agree with those of the other on the boundary surface.

The following simultaneous integral equations whose unknown functions represent the electric fields on the boundary surface are reduced by the process described above.

$$
\left.\begin{aligned}
&f(\theta) + \int_0^{2\pi}\int_0^{d} E_Z(\varphi,\ z)G_{1\cdot1}(\varphi,\ z,\ \theta,\ Z)d\varphi dz \\
&\quad + \int_0^{2\pi}\int_0^{d} E_\theta(\varphi,\ z)G_{1\cdot2}(\varphi,\ z,\ \theta,\ Z)d\varphi dz = 0 \\
&\int_0^{2\pi}\int_0^{d} E_Z(\varphi,\ z)G_{2\cdot1}(\varphi,\ z,\ \theta,\ Z)d\varphi dz \\
&\quad + \int_0^{2\pi}\int_0^{d} E_\theta(\varphi,\ z)G_{2\cdot2}(\varphi,\ z,\ \theta,\ Z)d\varphi dz = 0\,,
\end{aligned}\right\} \qquad (30)
$$

where

$f(\theta)$: The term determined by the primary field.

$E_Z(\theta,\ Z)$, $E_\theta(\theta,\ Z)$: The tangential electric field components on the boundary surface in question

** The potential waves, $m>0$, in U_{I} and U_{I}^{*} are all attenuated waves and the quantites of their image waves in the guide are very small, so we will neglect them in the later calculation, for simplicity.

and $G_{1\cdot1}(\varphi, z, \theta, Z)$, ……, $G_{2\cdot2}(\varphi, z, \theta, Z)$: the kernel of the integral equations which satisfy the boundary conditions.

To solve this simultaneous integral equation, we expand both of the unknown functions, $E_Z(\varphi, z, \theta, Z)$, $E_c(\varphi, z, \theta, Z)$ and kernel $G_{1\cdot1}$, ……, $G_{2\cdot2}$ into the Fourier series in the domain of the boundary surface, expansion coefficients of $E_Z(\varphi, z, \theta, Z)$, $E_\theta(\varphi, z, \theta, Z)$ are unknown, however.

Then the simultaneous linear equations of the expansion coefficients are reduced by using the nature of orthogonality of the integration of Eq. (30).

Solution of these equations determines the unknown fields, E_Z, E_θ.

From them, the reflection and transmission coefficients based upon the disturbance by a post are obtained in the same way as is described and its equivalent T network is introduced as follows by Eq. (19).

The values of M.N in this case are represented as follows.

$$M = -\frac{\pi a}{2\lambda_g}\left[\frac{Y_0(\kappa\rho)}{J_0(\kappa\rho)} + 2Y_{\tilde{0}}(\kappa a) + \frac{2}{\pi\rho\{\kappa(b/d-1)J_0(\kappa\rho)J_1(\kappa\rho)+2\pi bF_0J_0(\kappa\rho)^2\}}\right] \tag{31}$$

$$N = -\frac{\pi\lambda_g a}{4\lambda^2}\left[\frac{Y_1(\kappa\rho)}{J_1(\kappa\rho)} + 2Y_{\tilde{2}}(\kappa a) + 2Y_{\tilde{0}}(\kappa a) + \frac{2}{\pi\rho\left[\kappa(1-b/d)J_1(\kappa\rho)\{J_0(\kappa\rho)-\frac{1}{\kappa\rho}\cdot J_1(\kappa\rho)\}+\pi bF_1J_1(\kappa\rho)^2\right]}\right], \tag{32}$$

where

$$F_0 = \frac{\kappa^2}{\pi b}\sum_{m=1}^{\infty}\frac{\kappa_1(k_{rm}\rho)}{k_{rm}\kappa_0(k_{rm}\rho)}\left\{\frac{\sin\frac{m\pi}{b}d}{\frac{m\pi}{b}d}\right\}^2 \tag{33}$$

$$F_1 = \frac{2}{\pi b\rho}\sum_{m=1}^{\infty}\frac{\kappa_1^2(k_{rm}\rho)-\kappa^2\rho^2\kappa_0(k_{rm}\rho)\kappa_2(k_{rm}\rho)}{\kappa_1^2(k_{rm}\rho)-k_{rm}\rho\kappa_1(k_{rm}\rho)\kappa_2(k_{rm}\rho)}\left\{\frac{\sin\frac{m\pi}{b}d}{\frac{m\pi}{b}d}\right\}^2 \tag{34}$$

$$k_{rm} = \sqrt{\left(\frac{m\pi}{b}\right)^2-\kappa^2}, \quad \kappa_n(k_{rm}\rho)\text{: A modified Bessel}$$

function of the nth order of the 2nd. kind.

In Fig. 2.10 the values of the theoretical calculation by using above equations are compared with the corresponding experimental values.

In case of the very narrow gap, the values of the shunt element can be obtained by adding the supplemental term to the value of the case when the gap is closed.

Then if we denote Q as the transformation coefficient, $Z_c/Z_{\text{equi.}c}$, where $Z_{\text{equi.}c}$ is the equivalent network value of the gap and Z_c is the capacitance of the gap, we get the following equation.

$$Q = \frac{Z_c}{Z_{\text{equi.}c}} \simeq \left[\left\{\frac{2(b-d)}{\pi\rho a}J_0(\kappa\rho)J_1(\kappa\rho)\right\}\left\{1+\frac{2\pi bF_0J_0}{(\kappa\rho)(b/d-1)\kappa J_1(\kappa\rho)}\right\}\right]. \tag{35}$$

This equation gives the transformation relation between the gap capacity and the

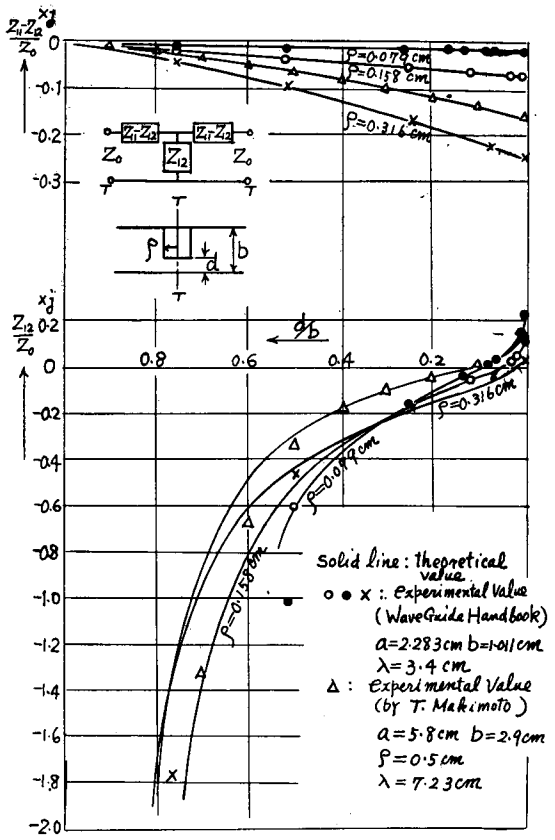

Fig. 2.10. The comparison between the theoretical and experimental equivalent circuit values of the metallic post.

corresponding constant of its line equivalent circuit, normalized by the characteristic impedance of the wave guide and this relation is useful for the separation of the electronic admittance from the measured values by mean of a wave guide rather a cavity.

The numerical example of this transformation coefficient, Q is shown in Fig. 2.11.

Conclusions

The theoretical studies of microwave circuits treated in this paper are concerned with the boundary value problems of discontinuities of a junction of the wave guide.

First, with respect to the junction problem of circular wave guides of the different radii, we used a simple but very convenient method by which we can solve the integral equation approximately. But the equivalent circuit representations obtained are very distinct in the physical explanation.

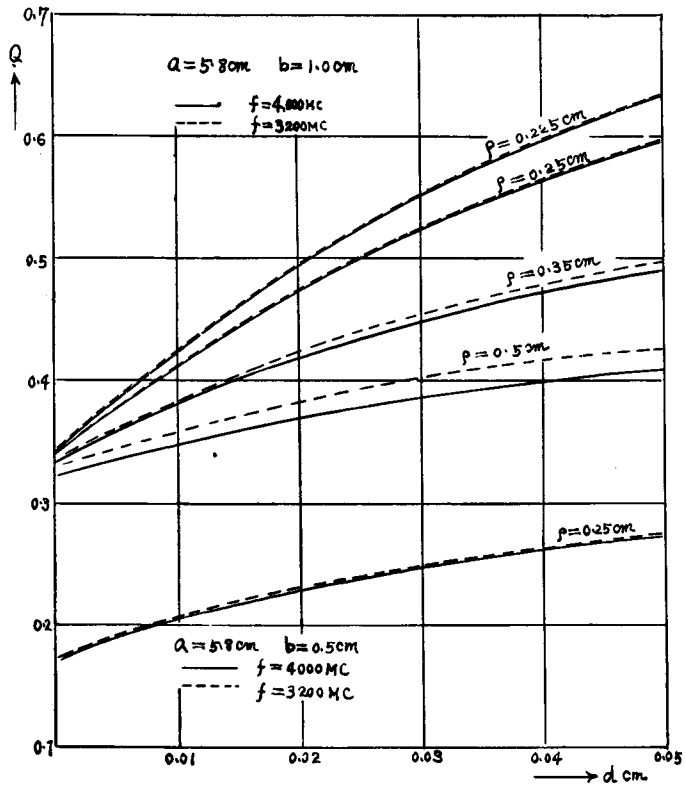

Fig. 2.11. The calculated examples of transformation coefficient, Q.

Next, some cases of a rather fat cylinder inserted into the wave guides are treated by using the principle of the image method.

These characteristics could be explained by the corresponding equivalent circuit representations.

These results have given the theoretical foundations for the measurement of the electric admittance of the tube with a very narrow electrode spacing by waveguide method.

References

1) H. A. Bethe: Theory of Diffraction by small Holes. Phys. Rev. Vol. 66 Oct. 1944.
2) T. Kato: Approximate Calculation by the Variational Method. Joul. of Phys. Soc. of Japan Vol. 6 No. 1.
3) M. Goto: Characteristics of Circular Cylinder in Rectangular Wave-guide. The Materials for the Research of E. C. L. of Japan. No. 11 Nov. 1950.